Reducing Uncertainty in Multi-Robot Construction through Perception Modelling and Adaptive Fabrication

D. Ruan[1], W. McGee[1], and A. Adel[1*]

[1]University of Michigan, USA
[*]Corresponding Author
deltar@umich.edu, wesmcgee@umich.edu, aaadel@umich.edu

Abstract

One of the significant challenges for robotic construction with dimensional lumber and other construction materials is the accumulation of material imperfections and manufacturing inaccuracies, resulting in significant deviations between the as-built structure and its digital twin. This paper presents and evaluates methods for addressing these challenges to enable a multi-robot construction process that adaptively updates future fabrication steps to accommodate for perceived inaccuracies, improving build quality. We demonstrate through a physical stacking case study experiment that our methods can decrease fabrication deviations due to setup and calibration errors by utilizing robot perception and adaptive processes. Overall, this research advances current toolpath and task optimization strategies to help shape a comprehensive system for working with tolerance-aware robotic construction.

Keywords –

Robotic Assembly, Adaptive Fabrication, Perception, Timber Structures, Multi-Robot Construction

1 Introduction

Robotic construction with dimensional lumber and other construction materials imposes significant challenges for robotic systems due to material imperfections and fabrication tolerances [1], [2]. Depending on the quality of the lumber (e.g., grade 2 or 3), the cross-sections of elements could deviate from nominal values. Furthermore, due to the length of the full-height elements (e.g., 3 m), lumber elements are usually not completely straight and include considerable deformations (e.g., twists and bends), contributing to their positioning errors. Compounding these issues, wood can shrink and expand due to temperature and moisture variability. Material imperfections and manufacturing inaccuracies accumulate during the assembly process, resulting in a significant deviation between the as-built structure and its digital twin. Our previous experiments have shown deviations up to 60 mm while assembling a light timber wall assembly, and due to these inaccuracies, the automated process often must be interrupted and errors addressed manually, decreasing build quality and increasing time taken for fabrication.

The current challenge in autonomous manufacturing and assembly of building-scale structures is the high intrinsic complexity of construction tasks and the lack of human-robot interfaces designed for the specific operational needs of construction [3]. This is in part due to the adoption of robotic systems from other industries such as the automotive industry, which operates in a highly structured and repetitive environment. Through the integration of more intelligent perception, reasoning, and control algorithms, a streamlined digital design-to-fabrication workflow can better address potential unforeseen collisions and part imprecisions, especially when compounded with the challenge of operating multiple robots cooperatively. This paper presents and evaluates methods for addressing the discussed challenges to enable a multi-robot construction process that adaptively updates future fabrication steps to accommodate for perceived inaccuracies due to material imperfections and manufacturing inaccuracies, improving build quality.

2 Related Work

Multi-robot systems have long been established for assembly line applications, with well-synchronized repetitive tasks [4], [5]. Cooperative robotic fabrication for construction, however, is still being explored, with applications including foam wire cutting [6], masonry vault construction [7], spatial metal structure assembly [8], and timber construction [1], [9]–[15]. In addition to distributing workload, robotic cooperation can also be utilized to perform construction tasks that cannot be achieved by a single robot, as is often the case when working with spatial assemblies.
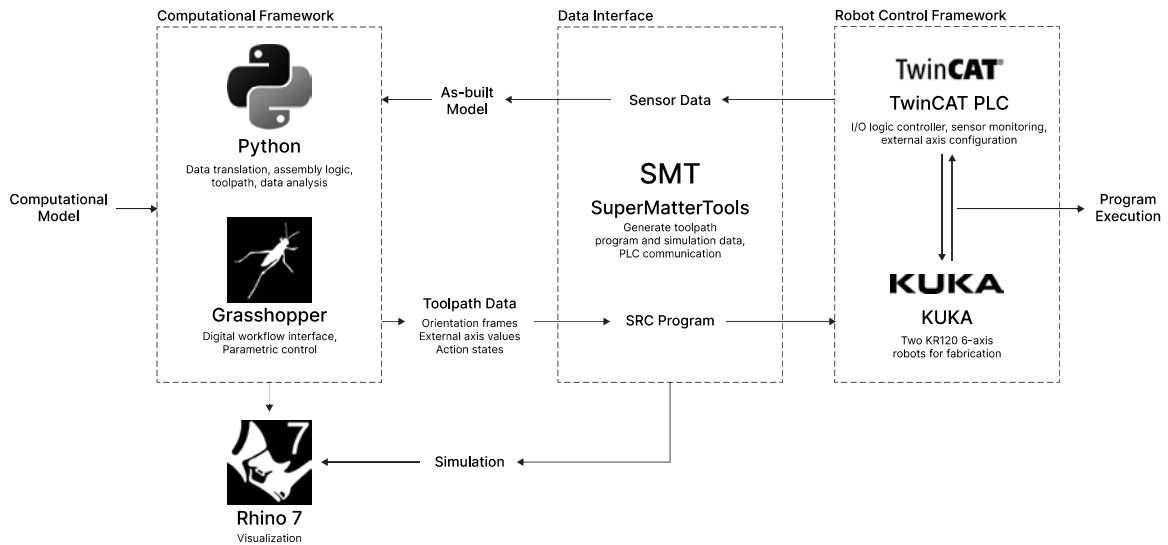
Figure 1. Digital design to fabrication workflow, highlighting the transfer of data between the computational model and the robot, adapted from previous research [9].

Focusing specifically on light timber assembly, the tight tolerances required for structural integrity coupled with the imperfect nature of timber studs make fully automated assembly challenging. The calibration of the robots and their tooling becomes a critical factor in determining as-built tolerances, with the real possibility of failure due to part collision. An end-effector positioning system utilizing static and dynamic correction through external pose tracking can reduce average positioning error down to 0.10 mm [16]; however, this solution has limited application outside of a defined workspace and is not suitable for adapting to material and process deviations.

There has been research to develop methods for dynamically adapting to these deviations. Gandia et al. [2] present a tolerance-aware computational design method for spatial timber structures, demonstrating how an optimal assembly sequence can be generated to minimize propagated tolerances. Eversmann et al. [17] use scanning to calculate the gripping and placement of differently sized shingles, however there was no feedback for updating post-placement tolerances, presumably due to the flexibility of a shingle system. Devadass et al. [18] reference a haptic fiducial to dynamically calibrate the workpiece cutting process for a mobile robotic setup, although assembly was still assisted through human robot collaboration. These approaches focus on minimizing tolerances during material processing and design computation, and as such there exists a gap in current literature on how to address deviations during the fabrication and assembly steps.

Adaptive fabrication techniques have long been embedded into the culture of craft, overcoming materials and environments with uncertain conditions by utilizing visual and haptic perception to inform decision-making in real-time [19]. When translated to robotic processes, computer vision technologies such as three-dimensional (3D) laser scanning and force/torque sensing form a basis for robotic perception, which then informs how the robot reasons with its surroundings to perform its next action in a feedback loop.

Recent research has demonstrated the application of adaptive robotic subtractive manufacturing processes for stone carving [19] and wood [20], where the visualization and predictive techniques afforded by adaptive processes enable human-like responsiveness towards working with the material. Adaptive processes have also been utilized for the localization and calibration of a mobile robotic fabrication system for building-scale mesh welding [21], increasing accuracy through continuous mapping of the environment and surveying of the fabrication process.

Overall, the main objective of this research is to develop and evaluate adaptive assembly techniques that enable cooperative multi-robot timber assembly by minimizing positional and process deviations, as well as handling material imperfections. These adaptive techniques will be evaluated through a set of physical stacking experiments to determine their effectiveness based on fabrication tolerance metrics.

3 Methods

3.1 Fabrication Setup

The fabrication testbed for this research consists of two KUKA [22] KR 120 R2700 6-axis industrial robot arms, named 'North' and 'South', mounted on parallel linear tracks, which allows full access to a raised
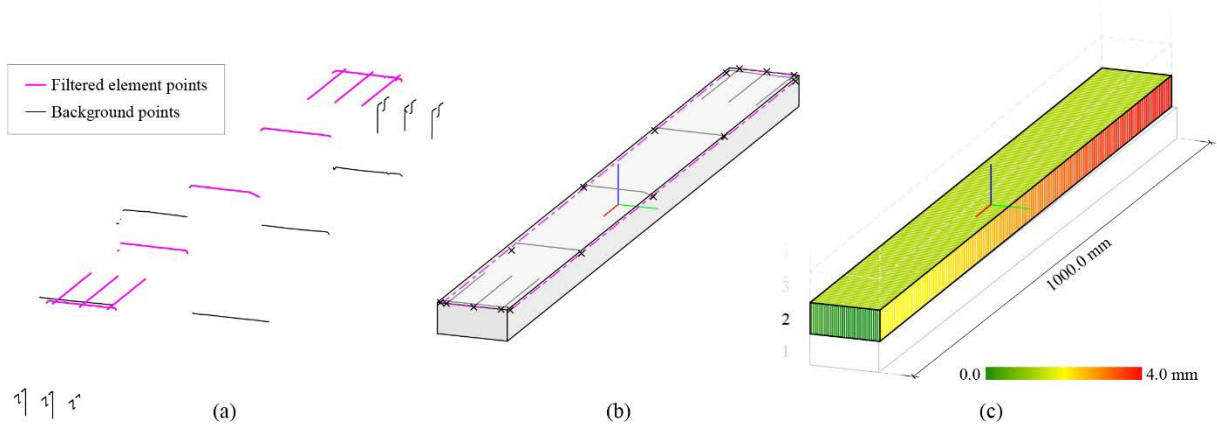
Figure 2. The scan processing begins with filtering the profile pointcloud (a), isolating the points scanned from the top face of the element. The filtered profiles are then used to generate a geometric representation and its central frame (b). The as-built model is updated with the newest element, which can be used to calculate deviations from the digital model (c).

assembly platform and a custom 3-axis computer numerical controlled (CNC) table saw. Each robot is equipped with a pneumatically controlled gripper end effector, which can be swapped out for an LMI Technologies Gocator 2350 [23] two-dimensional (2D) laser profiler for all scanning operations. Control of the workcell and collection of sensor data is processed through a programmable logic controller (PLC, Beckhoff TwinCAT [24]).

3.2 Timber Assembly Process

The basic timber assembly process, as the main case study process for this research, starts with a human operator loading a standard 2x4 piece of lumber down the center of the saw table, with one end roughly aligned with the edge of the table. The active robot then picks up the raw stock and performs two cuts on the saw for the model-specified length and end-plane angles. The gripping frame is located on the stock such that the first cut safely minimizes offcut volume, while the second cut maximizes the remaining material for future cuts, also making sure to avoid any potential collision between the saw blade and the gripper. Without regripping, the cut 2x4 element is brought over to the assembly platform and inserted into its final position within the sub-assembly. The human operator then fastens the element into place (e.g., with screws to previously placed elements, or with clamps if directly attached to the platform) before the robot releases the element and retracts. This process repeats until the sub-assembly is complete.

3.3 Digital Design-to-Fabrication Workflow

We have adapted a digital design-to-fabrication workflow based on previous research [9], which integrates Rhinoceros 3D [25], its plugin Grasshopper [26] and Python [27] with Super Matter Tools [28], a custom computational design tool for offline

programming and simulation (see Figure 1). This workflow enables a seamless connection between the digital design of the fabrication module and the robotic simulation, control, and manufacturing.

The forward loop of the workflow translates each timber element's modelled geometry into frames (consisting of position and orientation) that can be interpreted by our control algorithm for path planning. The primary frame for each element is chosen to be located at the centroid of the element, aligned with its long axis, ensuring safe and stable gripping while cutting and placing the element during assembly. Cutting attributes (such as cutting distance, saw blade angles) are generated parametrically from the modelled end planes. The pickup and saw locations are taught, while the path traversal and gripping states are configured prior to fabrication. All of these parameters are then automatically post-processed into Kuka Robot Language (KRL) to be executed by the robot.

The backward loop of the workflow enables feedback into the digital design loop, allowing for alterations to the model based on observed as-built conditions. This loop is what enables the adaptive adjustment of model parameters to reduce deviations in the fabricated sub-assembly.

Perception of the workpiece occurs both before and after each pick-cut-place operation to assist in the adaptive processes, as discussed in the following section. At this point in the process, the active robot swaps to the laser profile scanning end effector and performs a series of profile scans of the placed element to generate a digital as-built model. Profile scanning was selected over sweep scanning due to its minimal memory and processing requirements, while still being able to capture the critical boundary points to reconstruct the element digitally within reasonable accuracy. The reconstructed element is then used to update the as-built model, which can be compared with the original model to perceive deviations (see Figure 2).

3.4 Adaptive Processes

In order to reduce deviations between the digital and as-built models, we introduce adaptation into the fabrication workflow. Adaptation is enabled through the robots' usage of the laser profile scanner, which defines a perceptual coordinate space model in relation to the base world coordinate system for each robot. This process utilizes the physically placed elements as an anchor point to align the digital model with the perceptual spaces of each robot.

Two adaptation steps are added to the fabrication process – in the first, the active robot scans the previously placed element to determine the current deviation and estimate the correction (i.e., changes placement position and orientation) required to minimize deviations in the next element. After placing the next element, the active robot scans the new element to evaluate and update its estimation model.

The true as-built frame of a placed element in the world coordinate system is notated as p_n^W, where n is the element index. The relation between this true frame and the scanned frame is as follows:

$$p_n^L = T_{LW} \, p_n^W + \varepsilon_n^L \qquad (1)$$

Where p_n^L is the scanned frame relative to the robot laser's tool center point (TCP, T_{LW} is the transformation between the laser and world spaces, and ε_n^L is the measurement noise due to the scanning process. T_{LW} is, in turn, comprised of transformations from the scanner TCP to the robot flange (T_{LF}), robot flange to the robot root (T_{FR}), and robot root to the world (T_{RW}, see Equation (2)).

$$T_{LW} = T_{LF} \, T_{FR} \, T_{RW} \qquad (2)$$

Of these transformations, T_{LF} is calibrated by the user, T_{FR} is calculated by the robot controller and assumed to be accurate, leaving T_{RW} as the primary source of deviation between the laser and world spaces. This deviation is trivial in a single robot workcell with a fixed root, as the world space can be defined to be the same as the robot root. However, in a multi-robot workcell, any deviation in installation or calibration may result in a mismatch between each robot's perception of the world space. As an example, the two robots used in this paper have world spaces that are offset by approximately 4 mm, which translates to deviations in fabrication when operating without adaptation processes. To address this, one robot is arbitrarily chosen as the primary robot, setting the world space equal to its root (i.e., $T_{RW}^0 = I$). T_{RW} can then be estimated for the remaining robots $k \geq 1$ by relating their scanned element frame to the primary robot's.

$$\hat{T}_{RWn}^k = \underbrace{(T_{LF}^k \, T_{FR}^k)^{-1} \, p_n^{Lk}}_{\text{robot k}} \, \underbrace{[(T_{LF}^0 \, T_{FR}^0)^{-1} \, p_n^{L0}]^{-1}}_{\text{primary robot}} \qquad (3)$$

As the number of elements increases, $\hat{T}_{RW}^k$ is refined through linear least squares approximation. With a model for the transformation between the robot's perceptual space the world space, an estimate of the true as-built frame can be derived from Equation (4) and applied to determine the current deviation T_{WDn} between the digital and as-built models.

$$\hat{p}_n^W = T_{WDn} \, p_n^D \qquad (4)$$

This transformation is then applied to the modelled frame of the next element p_{n+1}^D alongside an estimated gripper error $\hat{T}_{GE}$ to obtain the gripper target position in the robot perceptual space $\dot{p}_{n+1}^R$ (see Equation (5)), which is input into the toolpath program generation.

$$\dot{p}_{n+1}^R = \hat{T}_{GEn} \, \hat{T}_{RWn} \, T_{WDn} \, p_{n+1}^D \qquad (5)$$

The gripper error is derived from the second adaptation step after placing and scanning the new element. This model is initialized (before the start of a fabrication task, for example) with a test piece assuming $T_{GE} = I$. With the post-placement scanned frame p_{n+1}^L, the gripper error is updated with linear least squares.

$$p_{n+1}^L = T_{LR} \left(\hat{T}_{GEn+1} \right)^{-1} \dot{p}_{n+1}^R + \varepsilon_{n+1}^P \qquad (6)$$

Where ε_{n+1}^P is the process noise error, which can result from material deformation, shifting while fastening, etc., assumed to have a mean of 0. Altogether, there is now a forward adaptation step for adjusting the position and orientation of the next element, as well as a backward adaptation step for evaluating and updating the error estimation model.

Adaptation can be applied in two ways in a multi-robot fabrication workflow – in the first, the arbitrarily designated primary robot does not incorporate any adaptation steps, and instead, the other robot(s) adapt and work around the primary robot. In this case, the primary robot establishes a ground truth throughout the fabrication process by adhering strictly to the digital model but is therefore reliant on its initial calibration to minimize deviations. The second method of adaptation is for all the robots to incorporate adaptation, which increases the primary robot's ability to respond to deviations at the cost of decreased protection against cumulative tolerances. To investigate the effectiveness of these adaptative processes, we conducted an experiment to compare the average deviation of a fabrication task with and without adaptation.

3.5 Experiment

The experiment was tasked with cutting and stacking ten 1000 mm lengths of standard 2x4 lumber from 8 ft (2.4 m) stock, alternating between the two robots of the experimental workcell, North and South, as the active robot. Although the model design is architecturally trivial,

the rotational alignment and positional accuracy of both robots is critical to the success of the task (i.e., forming a flat vertical wall), demonstrating the effectiveness of adaptation in a multi-robot fabrication setup. The effectiveness of the fabrication process was evaluated based on the average and per-element frame deviations.

The first experimental process was the base case, with no adaptation on either robot. In the second experimental process, North was set as the non-adapting primary robot while South adapted to its placements. In the third experimental process, both robots utilized adaptation. One stack of ten timber elements was fabricated for each of the three processes, generating ten sample points each (five per robot). Each sample point is a 6-dimensional vector (x, y, z, roll, pitch, yaw) representing an element's deviation (transformation) relative to its original modeled configuration frame. The results of the second and third processes are benchmarked with the base case.
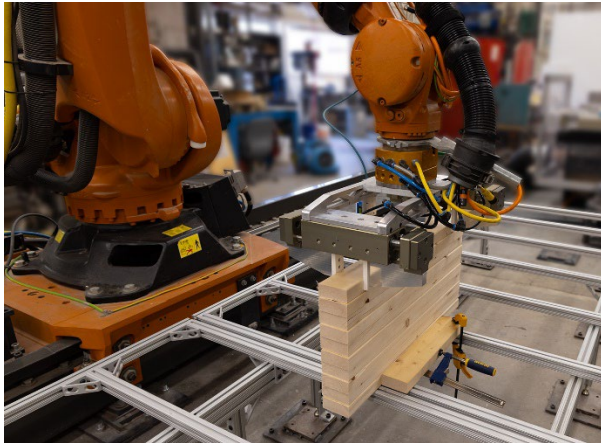

Figure 3. The South robot placing the final element in a timber stacking task (with no adaptation).

4 Results

Figures 4-6 plot the x and y components of each sample point across the three experimental processes. The perception of each robot (colored red for North, blue for South) is consistently offset for each process, indicating the base difference between the two robots' perceptual spaces. Within each perceptual space, the base case (Figure 4) highlights the calibration error between North-placed elements (circles) and South-placed elements (triangles), as the result of no adaptation, with the offset between the average deviation of each cluster being 2.5 mm. The average deviation of a cluster is calculated by averaging the Euclidean distance of each sample point to their respective reference frame (modeled element frame). The second process (Figure 5) shows a marked improvement with South's adaptation
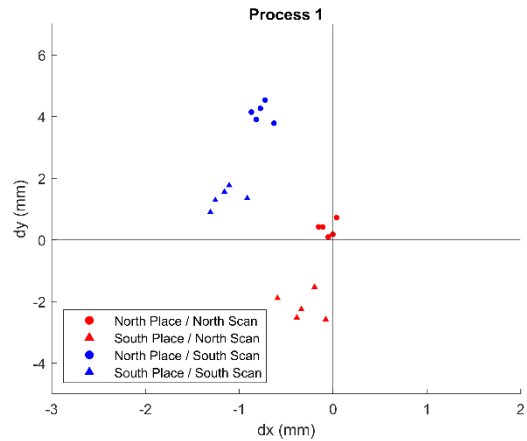

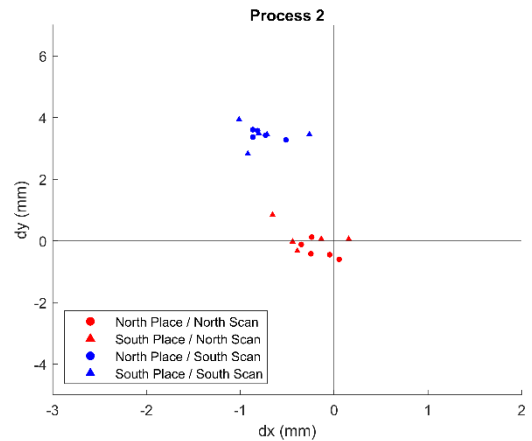Figure 4. XY frame deviation for Process 1 (base case), with no adaptation.

Figure 5. XY frame deviation for Process 2, with South adapting to North.
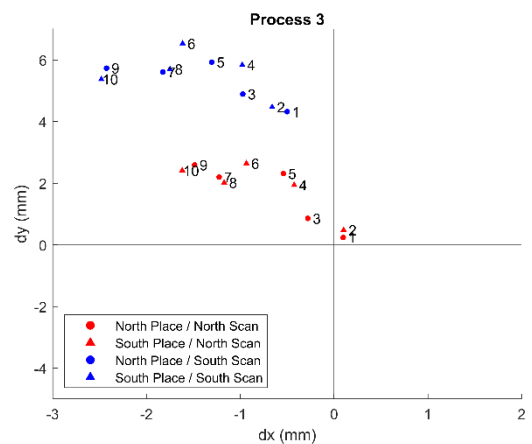

Figure 6. XY frame deviation for Process 3, with both North and South robots utilizing adaptation.

(a) Process 1
Base case - no adaptation

(b) Process 2
One robot adaptating

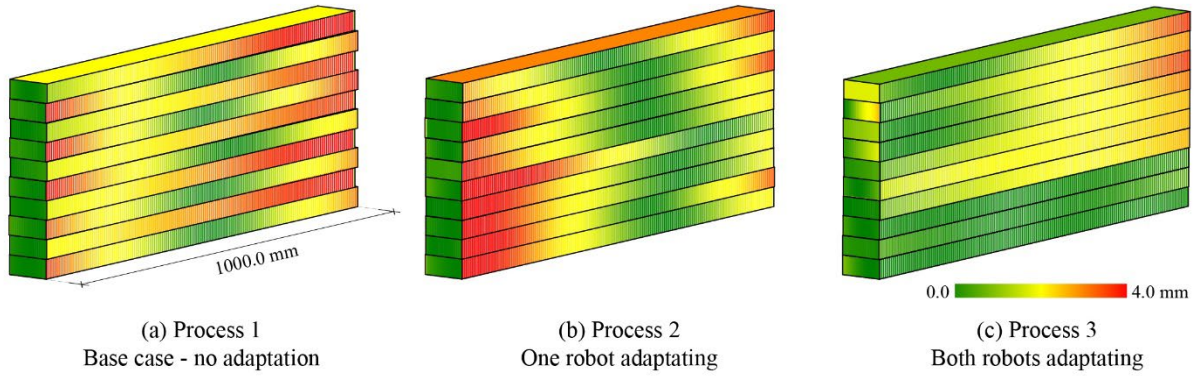(c) Process 3
Both robots adaptating

Figure 7. Heat maps indicating the deviations between the scanned and reconstructed as-built model and the digital blueprint model.

aligning its elements with North's, decreasing the offset to 0.4 mm and reducing the overall average deviation from 1.28 mm down to 0.45 mm (as measured by North).

The third experimental process shows the effect of cumulative deviations – each element in Figure 6 is labelled for legibility, with the elements having a clear drift direction, tending to deviate further from the modelled position as the task progresses. This is likely due to the fact that the two estimation models for the robot-world transformation $\hat{T}_{RW}$ and gripper error $\hat{T}_{GE}$ are still rough at the beginning of a new task, especially with the lack of an established ground truth as present in the case of the second process. Utilizing a larger initial dataset (e.g., gathered from previous tasks) could potentially alleviate most of this drift; however, more robust control logics are required to completely eliminate cumulative deviations.

Table 1. Element frame deviation translation (mm)

Process	Scanned by North		Scanned by South	
	Average	Stdev.	Average	Stdev.
1	1.28	1.01	3.00	1.28
2	0.45	0.26	3.53	0.28
3	1.96	1.03	5.66	0.77

Table 2. Element frame deviation rotation (°)

Process	Scanned by North		Scanned by South	
	Average	Stdev.	Average	Stdev.
1	0.107	0.255	0.108	0.263
2	0.377	0.053	0.354	0.055
3	0.484	0.086	0.452	0.090

5   Conclusion and Outlook

In this paper, we have introduced an adaptive process for multiple robots working cooperatively on a construction task. Initial experimental results demonstrate the potential for this adaptive process to decrease fabrication deviations due to setup and calibration errors by utilizing robot perception. The research also highlights future work to further refine the estimation models and cooperative fabrication workflow.

As next steps, we intend to apply the adaptive processes to light timber framed wall assembly tasks at building-scale as well as implement real-time control to drive the fabrication workflow. Part of this implementation will include a probabilistic model that accounts for the currently unaddressed measurement and process noise error terms. These advances will push the adaptive process in line with other current toolpath and task optimization strategies to create a comprehensive system for working with tolerance-aware robotic construction.

Acknowledgement

References

[1] Adel Ahmadian A. Computational Design for Cooperative Robotic Assembly of Nonstandard Timber Frame Buildings. ETH Zurich, 2020.
[2] Gandia A., Gramazio F., and Kohler M. Tolerance-aware Design of Robotically Assembled Spatial Structures. In *Proceedings of the 42nd Annual Conference of the Association for Computer Aided Design in Architecture (ACADIA),* 2022.
[3] Davila Delgado J. M., Oyedele L., Ajayi A., Akanbi L., Akinade O., Bilal M., and Owolabi H. Robotics and automated systems in construction:

Understanding industry-specific challenges for adoption. *Journal of Building Engineering*, 26100868, 2019.

[4] Dong Sun and Mills J. K. Adaptive synchronized control for coordination of multirobot assembly tasks. *IEEE Transactions on Robotics and Automation*, 18(4):498–510, 2002.

[5] Pellegrinelli S., Pedrocchi N., Tosatti L. M., Fischer A., and Tolio T. Multi-robot spot-welding cells for car-body assembly: Design and motion planning. *Robotics and Computer-Integrated Manufacturing*, 4497–116, 2017.

[6] Rust R. Spatial Wire Cutting: Integrated Design, Simulation and Force-adaptive Fabrication of Double Curved Formwork Components. ETH, Zurich, 2017.

[7] Parascho S., Han I. X., Walker S., Beghini A., Bruun E., and Adriaenssens S. Robotic vault: a cooperative robotic assembly method for brick vault construction. *Construction Robotics*, 4(3–4):117–126, 2020.

[8] Parascho S., Gandia A., Mirjan A., Gramazio F., and Kohler M. Cooperative Fabrication of Spatial Metal Structures. In *Fabricate 2017*, UCL Press, Apr. 05, 2017, 24–29.

[9] Adel A. Co-Robotic Assembly of Nonstandard Timber Structures. In *Proceedings of the 42nd Annual Conference of the Association for Computer Aided Design in Architecture (ACADIA)*, 2022.

[10] Thoma A., Jenny D., Helmreich M., Gandia A., Gramazio F., and Kohler M. Cooperative robotic fabrication of timber dowel assemblies. *Research culture in architecture*, 77–88, 2018.

[11] Craney R. and Adel A. Engrained Performance: Performance-Driven Computational Design of a Robotically Assembled Shingle Facade System. In *Proceedings of the 40th Annual Conference of the Association for Computer Aided Design in Architecture (ACADIA)*, 2020, 604–613.

[12] Wagner H. J., Alvarez M., Kyjanek O., Bhiri Z., Buck M., and Menges A. Flexible and transportable robotic timber construction platform – TIM. *Automation and Construction*, 120103400, 2020.

[13] Adel A., Thoma A., Helmreich M., Gramazio F., and Kohler M. Design of Robotically Fabricated Timber Frame Structures. In *Proceedings of the 38th Annual Conference of the Association for Computer Aided Design in Architecture (ACADIA)* 2018, 394–403.

[14] Graser K., Adel A., Baur M., Pont D. S., and Thoma A. Parallel Paths of Inquiry: Detailing for DFAB HOUSE. *Technology|Architecture + Design*, 5(1):38–43, 2021.

[15] Thoma A., Adel A., Helmreich M., Wehrle T., Gramazio F., and Kohler M. Robotic Fabrication of Bespoke Timber Frame Modules. In *Robotic Fabrication in Architecture, Art and Design 2018*, Cham: Springer International Publishing, 2018, 447–458.

[16] Stadelmann L., Sandy T., Thoma A., and Buchli J. End-Effector Pose Correction for Versatile Large-Scale Multi-Robotic Systems. *IEEE Robotics and Automation Letters*, 4(2):546–553, 2019.

[17] Eversmann P., Gramazio F., and Kohler M. Robotic prefabrication of timber structures: towards automated large-scale spatial assembly. *Construction Robotics*, 1(1–4):49–60, 2017.

[18] Devadass P., Stumm S., and Brell-Cokcan S. Adaptive Haptically Informed Assembly with Mobile Robots in Unstructured Environments. 2019.

[19] Shaked T., Bar-Sinai K. L., and Sprecher A. Adaptive robotic stone carving: Method, tools, and experiments. *Automation and Construction*, 129103809, 2021.

[20] Brugnaro G. and Hanna S. Adaptive Robotic Carving. In *Robotic Fabrication in Architecture, Art and Design 2018*, Cham: Springer International Publishing, 2019, 336–348.

[21] Dörfler K., Hack N., Sandy T., Giftthaler M., Lussi M., Walzer A., Buchli J., Gramazio F., and Kohler M. Mobile robotic fabrication beyond factory conditions: case study Mesh Mould wall of the DFAB HOUSE. *Construction Robotics*, 3(1–4):53–67, 2019.

[22] KUKA. https://www.kuka.com/en-us (accessed Mar. 30, 2023).

[23] LMI Technologies. Gocator 2300 series. https://lmi3d.com/series/gocator-2300-series/ (accessed Mar. 30, 2023).

[24] Beckhoff. TwinCAT automation software. https://www.beckhoff.com/en-us/products/automation/twincat/ (accessed Mar. 30, 2023).

[25] Robert McNeel & Associates. Rhinoceros 3D, version 7.0. https://www.rhino3d.com/ (accessed Mar. 30, 2023).

[26] Rutten D. and Robert McNeel & Associates. Grasshopper 3D. https://www.grasshopper3d.com/ (accessed Mar. 30, 2023).

[27] van Rossum G. and Drake F. L. Python 3 Reference Manual. Scotts Valley, CA, 2009.

[28] Pigram D. and McGee W. Formation embedded design. In *Proceedings of the 31st Annual Conference of the Association for Computer Aided Design in Architecture (ACADIA)*, 2011, 122–131.